Published in final edited form as:
J Neuroendocrinol. 2009 May ; 21(5): 506–517. doi:10.1111/j.1365-2826.2009.01860.x.

Age- and Hormone-Regulation of N-Methyl-D-Aspartate Receptor Subunit NR2b in the Anteroventral Periventricular Nucleus of the Female Rat:

Implications for Reproductive Senescence

J. A. Maffucci[*], **M. L. Noel**[†], **R. Gillette**[†], **D. Wu**[†], and **A. C. Gore**[*,†,‡]

[*]Institute for Neuroscience, University of Texas at Austin, Austin, TX, USA

[†]Division of Pharmacology and Toxicology, University of Texas at Austin, Austin, TX, USA

[‡]Institute for Cellular and Molecular Biology, University of Texas at Austin, Austin, TX, USA

Abstract

Glutamate, acting through its *N*-methyl-D-aspartate (NMDA) and non-NMDA receptors in the hypothalamus, regulates reproductive neuroendocrine functions via direct and indirect actions upon gonadotrophin-releasing hormone (GnRH) neurones. Previous studies indicate that the NMDA receptor subunit NR2b undergoes changes in protein and gene expression in the hypothalamus in general, and on GnRH neurones in particular, during reproductive ageing. In the present study, we examined whether the NR2b-expressing cell population, both alone and in association with the NR1 subunit (i.e. the latter subunit is necessary for a functional NMDA receptor), is altered as a function of age and/or steroid hormone treatment. Studies focused on the anteroventral periventricular (AVPV) nucleus of the hypothalamus, a region critically involved in the control of reproduction. Young (3-5 months), middle-aged (9-12 months), and aged (approximately 22 months) female rats were ovariectomised and, 1 month later, they were treated sequentially with oestradiol plus progesterone, oestradiol plus vehicle, or vehicle plus vehicle, then perfused. Quantitative stereologic analysis of NR2b-immunoreactive cell numbers in the AVPV showed an age-associated decrease in the density of NR2b-immunoreactive cells, but no effect of hormone treatment. In a second study, immunofluorescent double labelling of NR2b and NR1 was analysed by confocal microscopy of fraction volume, a semi-quantitative measure of fluorescence intensity. No effect of ageing was detected for immunofluorescent NR1 or NR2b alone, whereas the NR2b fraction volume increased in the oestradiol plus vehicle group. With ageing, the fraction volume of the NR2b/NR1-colocalised subunits increased. Together with the stereology results, this suggests that, although fewer cells express the NR2b subunit in the ageing AVPV, a greater percentage of these subunits are co-expressed with NR1. Our results suggest that the subunit composition of NMDA receptors in the AVPV undergo both age- and hormonal-regulation, which may be related to previous observations of changes in functional responses of reproductive neuroendocrine systems to NMDA receptor modulators with ageing.

Correspondence to: Dr Andrea C. Gore, Division of Pharmacology and Toxicology, The University of Texas at Austin, 1 University Station A1915, Austin, TX 78712, USA (e-mail: andrea.gore@mail.utexas.edu)..

Keywords

N-methyl-D-aspartate receptor (NMDA receptor); NR2b; reproductive ageing; oestrogen; gonadotrophin-releasing hormone (GnRH); glutamate

Excitatory amino acids such as glutamate are critical to the regulation of the hypothalamic-pituitary-gonadal axis. Glutamatergic *N*-methyl-D-aspartate (NMDA) and non-NMDA receptors are located throughout the hypothalamus and affect gonadotrophin-releasing hormone (GnRH) release directly, via expression on GnRH neurones, and/or indirectly via expression on neurones regulating GnRH release (1). The focus of this study is the NMDA receptor, which plays a physiological role in the regulation of the reproductive axis. Administration of NMDA receptor analogues excite, and antagonists inhibit, GnRH release *in vitro* and luteinising hormone (LH) release *in vivo* (1,2). Furthermore, these actions of glutamate on GnRH neurones are diminished with the onset of reproductive ageing (2,3), although the mechanisms behind these changes are yet to be identified.

The NMDA receptor is a heteromeric receptor composed of various combinations of the seven identified subunits (NR1, NR2a-d, NR3a-b). The NR1, NR2a and NR2b subunits are abundantly expressed in the hypothalamus in general and on GnRH cell bodies in particular, with evidence suggesting that these three subunits underlie many of the functional responses of GnRH neurones to NMDA receptor modulators (1,2,4-7). The NR1 subunit is obligatory for a functional channel, and the NR2 subunits contribute to the binding of glutamate and the channel properties of the receptor (8-11). In the hypothalamus, the more likely subunit compositions are thought to be NR1/NR2a, NR1/NR2b or NR1/NR2a/NR2b (12), which differ in their physiological channel properties (13).

During ageing, studies in rodents show that there is a loss of GnRH responsiveness to NMDA receptor analogues/antagonists, and this finding may relate to the decrements in GnRH/LH pulsatility and surge generation. Considering the importance of the NMDA receptor composition in determining channel kinetics, it is likely that age-associated changes to the subunit population of these receptors in the hypothalamus are involved in the onset of reproductive ageing in rats. Indeed, measurements of mRNA levels of NMDA receptor subunits in large macro-dissections of the hypothalamus have demonstrated both regional differences and steroid hormone modulation, effects that vary between the subunits (1,2). A further study focusing on protein expression of NMDA receptor subunits in the anteroventral periventricular nucleus (AVPV) showed an age-related decline in NR1 levels (14). The AVPV is an integration centre for somatosensory pathways that converge onto GnRH neurones (15) and plays a key regulatory role in the proper functioning of the GnRH/LH surge and oestrous cyclicity (16). Additionally, the AVPV shows high co-expression of oestrogen receptor alpha and NMDA receptors (specifically NR1), suggesting that it is a likely region for the interaction of oestradiol and glutamate signalling (7). Finally, the AVPV, together with associated periventricular regions referred to collectively as the rostral periventricular area of the third ventricle (RP3V), is strongly implicated as having direct inputs to GnRH neurones that play key roles in the mediation of oestradiol feedback (17,18).

The expression of the NR2b subunit appears to be key to the functionality of the population of hypothalamic NMDA receptors. Previous and ongoing studies in our laboratory demonstrate that the administration of the NR2b selective antagonist ifenprodil results in the upregulation of various parameters of LH pulsatile release in both young and middle-aged rats (19); it causes a disruption of the steroid-induced LH surge in middle-aged rats (J. A. Maffucci and A. C. Gore, unpublished data); and it differentially affects GnRH mRNA levels in young and middle-aged rats (19). These data suggest that the NR2b subunit,

specifically, plays an important regulatory role in two very important physiological aspects of the female reproductive system (i.e. GnRH/LH pulsatile release and GnRH/LH surge) and is subject to age-associated changes in expression levels.

The present study examined age-associated changes in the expression of the NR2b subunit in the AVPV of young, middle-aged and aged rats. In addition, the effects of steroid hormone treatment were evaluated. Hormones modulate the effects of NMDA receptor analogues/antagonists on the hypothalamic-pituitary-gonadal axis, a response that may differ with ageing, and which in turn may be the result of differences in the NMDA receptor subunit composition. First, changes in NR2b protein expression were quantified by stereology and brightfield microscopy. Second, age- and hormone-associated alterations in those NMDA receptors expressing NR1 and NR2b either singly- or doubly-labelled, were analysed using confocal microscopy.

Materials and methods

Animals

A total of 75 female Sprague-Dawley rats were used in the present study. Rats were purchased from The University of Texas at Austin Animal Resource Facility rat colony (Austin, TX, USA), which contains animals received and bred from Harlan Sprague-Dawley, Inc. (Houston, TX, USA). Animals were young (3-5 months), middle-aged (9-12 months) or aged (approximately 22 months). Young animals included both virgin and previously-bred females, middle-aged and aged animals contained retired breeders. No effect of breeding status has been shown in any parameters analysed in previous studies in our laboratory (20-22). Vaginal smears taken daily showed all young animals to be regularly cycling; middle-aged animals were irregularly cycling or acyclic (persistent oestrus); and aged animals were acyclic (persistent oestrus or persistent dioestrous). Animals were housed two to three per cage in a temperature controlled (21-22 °C) room under a 12 : 12 h light/dark cycle (lights on 07.00 h). They were given food (Purina Mills Rodent Diet 5LL2; Purina Mills, St. Louis, MO, USA) and water *ad lib*. Cages received 8cm long PVC pipes for enrichment. All animal protocols were conducted in accordance with the Guide for the Care and Use of Laboratory Animals (23) in accordance with protocols approved by The University of Texas at Austin Institutional Animal Care and Use Committee.

Surgery

All rats were bilaterally overiectomised (OVX) under isoflurane anaesthesia between 09.00 and 12.00 h. Cycling (both regularly and irregularly) animals were OVX on diestrus. Rats were treated post-operatively with 5 mg/kg of Rimadyl (Henry Schein, Melville, NY, USA). Four weeks later, at 10.00 h, animals were s.c. implanted with a Silastic capsule (inner diameter 1.96 mm; outer diameter 3.18 mm) containing either 5% 17β-oestradiol/95% cholesterol or 100% cholesterol (both from Sigma-Aldrich, St Louis, MO, USA) as the vehicle, under isoflurane anaesthesia. Capsules were soaked in 0.9% saline at 4 °C for at least 24 h prior to implantation. Young, middle-aged, and aged animals received an implant 1.0, 1.5 or 2.0 cm in length, respectively. Different lengths were used to account for body weight increases with ageing. These capsule lengths and steroid hormone concentration have previously been shown to restore circulating oestradiol levels comparable to those of the pro-oestrus, young rat in all three age groups (22,24). Unfortunately, as a result of contamination of the post-mortem serum samples with oestradiol, we were unable to obtain oestradiol levels by our radioimmunoassay, but other oestrogen-sensitive parameters in these OVX rats (serum LH, uterine and pituitary size) confirmed that the oestradiol groups had appropriate physiological responses to oestradiol treatment, and that these were absent in the vehicle groups. In addition, carcasses were examined to ensure complete removal of all

ovarian tissues. After surgery, animals were housed individually. Two days later, at 10.00 h, half of the animals received an s.c. injection of progesterone (Sigma-Aldrich) dissolved in ethanol and diluted in sesame oil (0.59 mg), a dose sufficient to induce the steroid hormone induced LH surge (21,25). The remaining animals received a vehicle control injection (sesame oil). Twenty-four hours later, rats were deeply aenesthetised with 0.4 ml of ketamine (100 mg/ml) and 0.4 ml of xylazine (20 mg/ml). Blood was collected via cardiac puncture and animals were then perfused at a rate of 50 ml/min with 1% paraformaldehyde, followed by 4% paraformaldehyde, 0.125% glutaraldehyde in phosphate-buffered saline (PBS). After perfusion, the animals were examined for any signs of morbidity. Pituitary glands and uteri were removed post-mortem; pituitaries were weighed and uterine diameter was measured to assess the uterotrophic response to oestradiol. Bloods were allowed to clot, then centrifuged at 5000 × *g* at 4 °C. Serum was separated and stored at -80 °C for future hormone assays. Brains were removed from the skull and tissues post-fixed in 4% paraformaldehyde, 0.125% glutaraldehyde overnight at 4 °C. They were then sectioned coronally (40 μm) on a Vibratome (VT 1000S; Leica Instruments, Nussloch, Germany) and stored in PBS with 0.1% sodium azide at 4 °C.

Radioimmunoassay (RIA)

When possible, serum from each animal was assayed for concentrations of LH, oestradiol, and progesterone levels. However, in some cases, either insufficient or no serum could be collected to test for these levels. Additionally, assay results with a coefficient of variance > 10% between samples were excluded, as were statistically significant outliers determined by box-plot graphs used to identify outliers, and then verified using the Grubb's test for outliers (26). As noted above, the serum samples taken post-mortem were inadvertently exposed to oestradiol. This did not affect the outcomes of the LH and progesterone assays but caused serum oestradiol levels to appear higher than those expected for OVX rats. Therefore, the results of the oestradiol RIA are not shown. However, as shown in Tables 1 and 2, other post-mortem measurements taken on the rats confirm the efficacy of oestradiol treatment.

LH—Serum LH was determined in duplicate 50-μl samples in the laboratory of Dr Michael Woller (University of Wisconsin-Whitewater, Whitewater, WI, USA), using double-antibody RIA. This RIA was performed using the rat LH RP-3 standard, iodinate and an anti-rabbit antibody from the National Hormone and Pituitary Programme of the NIDDK (kindly provided by Dr A. F. Parlow, National Hormone and Pituitary Programme at NIDDK, Torrance, CA, USA). The primary antibody was complexed to goat anti-rabbit gamma globulin. The assay sensitivity was 0.03 ng/tube at 85% binding. The intra-assay variability was 2.36%.

Progesterone—Serum progesterone was determined in a coated tube RIA according to manufacturer's protocol (DSL-3900; Diagnostic Systems Laboratories, Inc., Webster, TX, USA). Samples (25 μl) were run in duplicate in a single assay. The sensitivity of this assay was 0.12 ng/ml and the intra-assay variability was 1.98%.

Immunohistochemistry for light microscopy

Tissue sections were taken at a 1 : 2 series across the AVPV. All steps were conducted on a shaking platform and at room temperature, with the exception of the primary antibody incubation that was conducted at 4 °C. Sections were washed in buffer (PBS). They were then treated to eliminate endogenous peroxidase (3 : 1 methanol: 3% hydrogen peroxide) for 15 min, rinsed in buffer, and incubated in 10% normal goat serum (S-1000; Vector Laboratories, Burlingame, CA, USA) and 0.1% bovine serum albumin (A9085; Sigma-Aldrich) for 1 h. Sections were incubated in rabbit anti-NMDA receptor-NR2b polyclonal antibody (0.2 μg/ml; NB 300-106; Novus Biologicals, Littleton, CO, USA) in 2% normal

goat serum for 3 days at 4 °C. The validation of this antibody has been previously described by Adams *et al.* (27). In that study, western blot analysis was performed across a panel of all NMDA receptor rat cDNAs transfected into HEK293 cells. This antibody recognised rat NR2b only at the appropriate molecular size of 180 kDa (27). In the present study, primary antibody was omitted in control sections. The sections were then incubated in 5% normal goat serum and biotinylated goat anti-rabbit immunogobulin (Ig)G (1 : 600; BA-1000; Vector Laboratories) for 1 h. They were then washed and incubated in avidin-biotin-peroxidase complex (PK 6200; Vector Laboratories) for 1 h, rinsed again, and developed in a diamino benzidene (DAB)/peroxidase reaction (SK-4100; Vector Laboratories). Sections were rinsed and mounted on gelatin-coated slides, dried, dehydrated in a graded alcohol series, counterstained with methyl green and coverslipped with DPX (44581; Fluka, Steinheim, Germany). As a result of the large number of tissues, multiple immunohistochemistry runs were performed, each containing tissues from at least one animal from each of the nine treatment groups, with similar numbers of animals per group.

Stereological analysis

Stereologic analysis was performed as described previously (14,28). Slides were recoded prior to analysis so that the investigator was blind to treatment groups. For stereological analysis, each AVPV region, counterstained with methyl green, was outlined at low magnification (× 4) on the live computer image by comparison to rat brain atlases (29,30). The AVPV was demarcated anterior to posterior using the crossing of the anterior commissure, with the anterior portion located at the level of the initial elongation and crossing of the anterior commissure, and the posterior region located at the completion of this crossing and the appearance of the rostral medial preoptic nucleus. A 100 × 1.4 numerical aperture objective was used to achieve optimal visualisation of labelled cells during analysis. Only animals with a complete AVPV series were quantified. Thus, several animals were excluded because of tissue damage, resulting in a final experimental sample size of young vehicle, vehicle (YVV) (n = 7); young oestradiol, vehicle (YOV) (n = 7); young oestradiol, progesterone (YOP) (n = 4); middle-aged vehicle, vehicle (MVV) (n = 7); middle-aged oestradiol, vehicle (MOV) (n = 6); middle-aged oestradiol, progesterone (MOP) (n = 8); aged vehicle, vehicle (AVV) (n = 7); aged oestradiol, vehicle (AOV) (n = 5); and aged, oestradiol, progesterone (AOP) (n = 5). The software package StereoInvestigator (Microbright-field, Colchester, VT, USA) was used to count labelled cells. The programme placed disector frames using a systematic, randomised sampling within each contour using a 60 × 125 μm grid. DAB-labelled NR2b cells were counted within the 45 × 45 μm optical disector frames on the x-y axis. The final post-processing thickness of the tissue was determined using the StereoInvestigator programme, and the average was determined to be 17 μm. The counting frame height was kept at 14 μm to stay within those limits and to allow a guard zone on the edge of the tissue where tissue may be uneven. Cells were counted using the optical fractionator and, as such, neuronal number estimates are not dependent upon the direct volume of reference of the region; thus, any shrinkage of tissue should not affect the quantification of labelled cells. Furthermore, the volume of the AVPV was determined via the outlining of the region at × 4, and multiplying this area by the total thickness and the inter-slice distance. Density of cells was calculated by dividing the extrapolated number of cells (as determined by the stereological analysis) by the volume of the AVPV. The coefficients of error and variation of the estimates were calculated as described previously (31). Gundersen's CE for the nine groups were: YVV = 0.09, YOV = 0.11, YOP = 0.09, MVV = 0.08, MOV = 0.11, MOP = 0.11, OVV = 0.10, MOV = 0.10 and MOP = 0.12.

Quantitative analyses were performed using a computer-assisted morphometry system including an Olympus photomicroscope (Olympus America, Centre Valley, PA, USA) equipped with a Ludl Precision2 MAC-5000XYZ computer-controlled motorised stage

(Hawthorne, NY, USA), and Optronics DC 100U digital camera (Goleta, CA, USA), a Dell computer (Austin, TX, USA), and StereoInvestigator morphometry and stereology software (Microbrightfield, Inc.). Stereological methods using the optical fractionator in Microbrightfield (32) were used to estimate the cell population of NR2b-immunoreactive cells in the AVPV. Labelled cells within the disector frames were counted on a live computer image at high power (× 100). The DAB staining of NR2b was easily distinguished from the methyl green counter-stain. Cytoplasmic membranes labelled for NR2b showed a brown cytoplasmic staining. The methyl green counterstain often labelled the nucleus in these cells, making it easily distinguishable from the DAB labelling pattern of NR2b immunoreactivity. Examples are provided in Fig. 1.

Immunofluorescence for confocal microscopy

Prior to experimentation, a range of primary and secondary antibodies were tested, along with appropriate controls (mentioned below) to optimise the reaction, to ascertain the sensitivity of the confocal microscope, and to minimise saturation effects. Tissue sections were taken at a 1 : 4 series across the AVPV of the same rats. All steps were again performed on a shaking platform and, with the exception of the primary antibody incubation performed at 4 °C, all other steps were done at room temperature (RT). Sections were first washed in buffer (PBS), then incubated in 10% normal goat serum (S-1000; Vector Laboratories) and 0.1% bovine serum albumin (A9085; Sigma-Aldrich) for 1 h. Sections were then incubated in rabbit anti-NMDA receptor-NR2b polyclonal antibody (0.2 μg/ml; NB 300-106; Novus Biologicals, Littleton, CO, USA) and mouse anti-NR1 antibody (5 μg/ml; 54.1 kindly provided by Dr John H. Morrison, Mount Sinai School of Medicine, NY, USA) in 2% normal goat serum for 3 days. Both of these antibodies have been validated as specific (27,33). Sections were then washed in buffer and incubated in 5% normal goat serum, anti-mouse Alexa-Flour 633 IgG (5 μg/ml; A-210-486; Invitrogen, Carlsbad, CA, USA) and anti-rabbit fluorescein isothiocyanate (FITC) IgG (3.33 μg/ml; F-2765; Invitrogen) for 1.5 h. Sections were washed, mounted on Superfrost Plus Premium microscope slides (12-550-15; Fisherbrand, Pittsburgh, PA, USA), dried, and coverslipped with Vectashield mounting media (H-1000; Vector Laboratories), and the coverslip perimeter sealed with clear nail polish. Sections were kept in low light to protect against photobleaching, and stored in the dark at 4 °C. Multiple controls were run: (i) primary antibody omitted; (ii) secondary antibody omitted; (iii) both primary and secondary antibodies omitted; (iv) NR2b primary antibody only; and (v) NR1 primary antibody only. No cellular or nuclear staining was detected in any of the controls, and the background was extremely low.

Confocal microscopic analysis

An SP2 AOBS Laser Scanning Confocal Microscope (Leica Microsystems Inc, Exton, PA, USA) was used to determine NR1 and NR2b expression and co-labelling in the AVPV. Subsections of the AVPV measuring 375 μm × 375 μm × 15 μm were imaged with a × 40 (1.25NA) objective at 1.00 zoom. Image stacks were acquired sequentially at excitation wavelengths of 488 and 633 nm and emission was collected in the range 500-510 nm for FITC-labelled NR2b and 640 and 680 nm for Alexa Fluor 633-labelled NR1 with a 1.0-μm z-axis step size. The 15-μm depth was chosen to ensure equal penetration of both antibodies across the entire scan. Scans were conducted over seven sequential days in order to minimise photobleaching of antibodies, and to avoid ‘drift’ in the confocal, with laser parameters remaining constant. Initial scans were performed in duplicate, using both a high and low laser setting to protect against saturating levels of immunofluorescence. At the end of day 1, it was determined that no saturation was present at the high laser setting and subsequent tissues were then scanned on this high setting only. At the start of each day, the last sample from the previous day was rescanned to control for possible shifts in the laser

readings. These were later compared using a paired t-test to determine any significant differences, of which there were none. In total, five regions were scanned over the three tissue sections, with one region encompassing the rostral AVPV slice, and two regions (one ventral and one dorsal) per each caudal AVPV slice (Fig. 2). At the caudal extent of the AVPV, other steroid-sensitive neurones of the rostral periventricular preoptic nucleus may be included, which acts together with the AVPV as part of the rostral periventricular area of the third ventricle that mediates positive feedback to GnRH neurones (18). Examples of immunofluorescence and co-expression are shown in Fig. 3.

IMARIS, version 5.7.0 (Bitplane Scientific Solutions, Zurich, Switzerland) was used to individually analyse scans in three dimensions. All scans were coded to keep treatment and age of each animal unknown. Sub-regions of 293 μm × 293 μm were analysed to exclude the third ventricle and the threshold levels were determined to subtract background autofluorescence. Co-localisation was determined using the IMARIS co-localisation algorithms. Volumes for NR1, NR2b and co-localisation were determined using the isosurface function and normalised to the volume of tissue analysed (858 490 μm^3).

The secondary antibody-only control was used to determine any nonspecific immunostaining. Alexa 633 showed no nonspecific labelling. FITC showed negligible labelling. This was determined by analysing the secondary only control (one section from a young, middle-aged and aged animal, respectively) using IMARIS, with the same parameters employed as used for experimental tissues. The average of the immunofluorescent volumes for these control tissues was taken and subtracted from the total volume of immunofluorescence of each experimental tissue. These totals were then compared wiith the unmodified FITC immunofluorescence data and no significant difference was determined. Therefore, the background immunolabelling had negligible effects on results.

Statistical analysis

Steroid hormones—Outliers were identified using a box-plot graph and excluded using the Grubb's outlier test (26). Two-way ANOVA was used to determine age-related differences in serum hormone levels and to verify differences in hormone treatments using SPSS, version 11 (SPSS Inc., Chicago, IL, USA) for Macintosh (variables: age and steroid hormone treatment). When indicated, post-hoc analysis was performed using Fisher's protected least significant difference test or Tukey's test. $P < 0.05$ was considered statistically significant.

Stereology—Variables were plotted on a box plot and possible outliers determined using the Grubb's outlier test (26) and excluded when confirmed. Two-way ANOVA was used to determine age and steroid hormone associated differences in the number and density of NR2b immunoreactive cells, as well as the volume of the AVPV. These were determined using SPSS, version 11 for Macintosh (variables: age and steroid hormone treatment). When indicated, post-hoc analysis was performed using Fisher's protected least significant difference test. $P < 0.05$ was considered statistically significant. No differences were observed in middle-aged females irregularly cycling prior to OVX ($n = 6$) compared to those in persistent oestrus ($n = 15$) and, thus, these groups were combined.

Confocal microscopy—Variables were plotted on a box plot and possible outliers determined. These were verified using the Grubb's outlier test (26) and excluded when confirmed. Comparisons of data acquired from different immunohistochemistry runs confirmed that datasets were overlapping, and by performing scans within a narrow time limit, the variability created by any drift in the laser was minimal. Two-way ANOVA was used to determine age and steroid hormone associated differences in the volume of NR1 and NR2b immunofluorescence, as well as the volume of NR1/NR2b colocalised

immunofluorescence. These were determined using SPSS, version 11 for Macintosh (variables: age and steroid hormone treatment). When indicated, post-hoc analysis using Fisher's protected least significant difference test was used. $P < 0.05$ was considered statistically significant. No differences were observed in middle-aged females irregularly cycling prior to OVX (n = 6) compared to those in persistent oestrus (n = 15) and, thus, these groups were combined.

Results

Stereologic analyses of changes in NR2b-immunoreactive cell number as a function of age or hormone treatment

Photomicrographs of NR2b-immunoreactive cells are shown in Fig. 1. Stereologic analyses showed that the number of NR2b immunoreactive cells in the AVPV did not change with age ($P = 0.188$) or hormone treatment ($P = 0.261$), nor was there any interaction among those variables ($P = 0.248$; data not shown). In addition, the AVPV volume did not change with age, hormone, or their interactions ($P = 0.501$, $P = 0.803$ and $P = 0.736$), respectively; data not shown). However, the density of NR2b immunoreactive cells within the AVPV decreased significantly as a function of age ($P = 0.017$; Fig. 4A), but not hormone treatment ($P = 0.162$; Fig. 4B). Young animals had a significantly higher density than aged ($P = 0.016$) and there was a trend for a decrease in density from middle-aged to aged animals ($P = 0.083$; Fig. 4A). There was a trend for interaction among the variables, but significance was not attained ($P = 0.059$; Fig. 4C).

Confocal analysis of changes in NR2b and NR1-immunofluorescence as a function of age or hormone treatment

Photomicrographs of immunofluorescent NR2b, NR1 and their co-expression are shown in Fig. 3. For NR1, there was no main effect of age ($P = 0.291$) or hormone treatment ($P = 0.740$) for the fraction volume of NR1 immunofluorescence, nor were there any interactions ($P = 0.863$; Fig. 5). For NR2b, there was also no main effect of age ($P = 0.832$) for the fraction volume of NR2b immunofluorescence (Fig. 6A). However, hormone treatment did cause an effect on this latter parameter ($P = 0.034$; Fig. 6B). Post-hoc analysis showed that animals treated with oestradiol plus vehicle had the highest fraction volume of NR2b-immunofluorescence compared to both the vehicle-vehicle and the oestradiol-progesterone groups (Fig. 6B). There was no interaction of age and hormone treatment on NR2b immunofluorescence ($P = 0.480$; Fig. 6C).

The colocalisation of NR2b with the NR1 subunit was examined. A main effect of age ($P = 0.029$; Fig. 7A), but not hormone treatment ($P = 0.107$; Fig. 7B), and no interaction of these variables ($P = 0.864$; Fig. 7C), was determined. Post-hoc analysis of the effect of ageing showed that colocalisation fraction volumes increased throughout the ageing process, with both young and middle-aged animals having significantly lower levels than aged rats ($P = 0.008$ and $P = 0.050$ respectively; Fig. 7A).

Additionally, although not quantified, it was noted during the analysis that a very high percentage of the NR2b immunofluorescent cells co-expressed the NR1 subunit at these optimised confocal scan settings. The converse (i.e. the percentage of NR1-expressing cells that co-expressed NR2b) was smaller. Together, these findings suggest that, whereas most NR2b-containing cells co-express NR1, not all NR1-containing cells express the NR2b subunit.

Serum hormone levels as a function of age or hormone treatment

Data presented for this and the subsequent part of the investigation are from animals whose tissues were used for this study, supplemented with some additional rats in the study that could not be used in our immunohistochemical analyses as a result of tissue damage or sample size requirements. Nevertheless, these additional animals were treated with the identical protocol and were used at the same time as the currently described cohorts. The inclusion of the additional animals was used to compensate for some lost or unusable serum samples from the animals used in the present study, aiming to increase the sample size.

Luteinising hormone—LH levels varied significantly as a function of both age ($P < 0.001$) and hormone ($P < 0.001$) treatment, with an interaction of these variables ($P < 0.001$) (Table 1) among all treatment groups. Young animals had higher LH levels than both middle-aged and aged ($P = 0.001$ and $P < 0.001$) and middle-aged animals were higher than aged ($P < 0.001$). A significant interaction of age and hormone was also detected ($P < 0.001$), with the young-vehicle/vehicle rats having significantly higher LH levels than all other groups.

Progesterone—As shown in Table 1, progesterone levels did not vary with age ($P = 0.840$), but were significantly different between hormone treatments ($P < 0.001$), with progesterone treated groups showing significantly higher levels than oestradiol only ($P = 0.014$) and vehicle only ($P < 0.001$) treated animals. There was no interaction between age and hormone treatment ($P = 0.890$).

Pituitary weights and uterine diameter as a function of age or hormone treatment

Pituitary weights—Pituitaries were removed and examined, and animals with observable tumors were excluded. Pituitary weights of healthy animals showed no differences with age ($P = 0.246$), and had an effect of hormone that approached but did not attain significance ($P = 0.051$; Table 2). Although post-hoc analyses were not performed, the pituitary weights of the vehicle/vehicle groups were consistently smaller than those in the oestradiol/vehicle and oestradiol/progesterone groups, as is expected for the oestradiol-induced pituitary cell hypertrophy (34-36).

Uterine diameter—Uterine diameter measurements showed no effect of ageing ($P = 0.890$), but a significant main effect of hormone treatment ($P < 0.001$; Table 2). Uterine weights could not be taken, as the ovariectomy procedure includes removing a portion of the uterus. Thus uterine diameter is a more accurate representation of the uterotrophic response to oestradiol treatment. Animals treated with oestradiol/vehicle or oestradiol/progesterone had significantly higher uterine diameters than those receiving vehicle ($P < 0.001$), and did not differ from one another ($P = 0.890$; Table 2). In addition, it was noted that all animals receiving oestradiol treatment had an enlarged, fluid-filled uteri compared to animals receiving vehicle alone, as previously reported (36,37).

Discussion

The present study was undertaken to determine whether changes to the NMDA receptor in the AVPV of the hypothalamus occur with reproductive senescence. The AVPV is a sexually dimorphic nucleus in the preoptic area that is important to the proper maintenance of female reproductive physiology via integration of GnRH neurones, steroid hormone and neuromodulatory signals (7,15,16). In addition, the AVPV is part of an integrated preoptic circuit termed the RP3V, which comprises the AVPV and the median and periventricular preoptic nuclei, which are crucial to oestrogen-sensitive control of positive feedback to GnRH neurones (18). This present study specifically examined age- and hormone-specific

changes to the expression of the NR2b subunit of the NMDA receptor based on evidence that this subunit is particularly likely to undergo changes with ageing, both on GnRH neurones and in surrounding hypothalamic regions (20,24,38). We also analysed the co-expression of NR2b with the NR1 subunit, because a functional channel containing NR2b also requires the co-expression of the NR1 subunit (39).

Age-associated changes in NMDA receptor subunits, and implications of receptor stoichiometry on physiology

Overall, our results suggest that NMDA receptor subunits in the AVPV undergo age-associated alterations. Stereologic counting of numbers of NR2b-immunoreactive cells in the AVPV showed that the density of immunoreactive NR2b cells decreased (by approximately 17%) from young to aged animals. In addition, an age-associated increase in NR1/NR2b colocalisation was observed, with young and middle-aged rats having a lower immunofluorescent fraction volume than aged animals. However, NR1 and NR2b immunofluorescence alone showed no age-associated change. Together, these data indicate that, although the overall number of cells expressing NR2b in the AVPV (by stereology) decreases with age, the volume fraction of the AVPV containing co-expressed NR2b with NR1 (by immunofluorescence) increases with age. The fraction volume is indicative of the amount of immunofluorescent labelling of protein within the volume of tissue scanned, as opposed to that of a stereologic analysis, which indicates the number of cells reacting. Thus, these data compliment one another, and we interpret them collectively to represent an increase in the amount of NR2b protein expressed per cell with a decrease in the total number of cells expressing this subunit. As a whole, our results suggest that there are changes in the NMDA receptor stoichiometry in the AVPV with ageing.

The available literature supports the idea that a functional NMDA receptor must contain both NR1 and NR2 subunits (9,10). Luo *et al.* (40) demonstrated that there are no NR2a/NR2b containing complexes that do not also contain NR1 in the adult rat cortex. In the present study, we observed that the vast majority of NR2b-containing cells are co-expressed with NR1, implying that, in the AVPV, most NR2b-containing cells have the potential to be functional NMDA receptors. Thus, age-associated changes to the NMDA receptor stoichiometry in this region have physiological consequences, and the ability of these NMDA receptors to bind to glutamate and to generate an intracellular signal are likely to differ in the ageing compared to the young AVPV, as a result of intrinsic differences in receptor subunit composition.

It has previously been shown that the composition of NMDA receptor subunits varies with age and brain region. In the adult rat cortex, the most abundant stoichiometry of the NMDA receptor contained at least three different subunits, NR1, NR2a, and NR2b (40). Although this has not been shown in the hypothalamus, should this be the case, the findings obtained in the present study suggest a possible switch from this preferred receptor stoichiometry in the young adult, to one in which NR1/NR2b is more prevalent. To determine this more conclusively, an analysis of NR1/NR2a co-expression is needed. Previous studies from our laboratory that analysed gene expression of NR1, NR2a and NR2b in the entire preoptic area, of which the AVPV is a small part, showed age- and hormonal-regulation (24), consistent with a change in stoichiometry. It will be interesting to investigate protein expression of NR2a, aiming to complement the current studies on NR2b and NR1. Although the tissues from this cohort of ageing rats were exhausted for the present analysis, we intend to pursue this avenue of research in future studies.

The implications of our finding for a change in the NR1/NR2b configuration in the AVPV with ageing include the possibility that the channel properties of this receptor undergo physiological alterations. The NMDA receptor mediates calcium signalling, which in turn

determines the probability that the channel will open. The NR1/NR2a stoichiometry has a much higher channel open probability than an NR1/NR2b containing channel (11,41). These channels undergo multiple conformational changes prior to opening, and at least one of these is faster in the NR2a containing channel than the NR2b. Thus, the signalling profiles for these channels are very different (41). Furthermore, rapid application of glutamate results in a slower deactivation time and slower recovery from desensitisation of NR1/NR2b containing receptors compared to NR1/NR2a (13). Finally, excitatory post-synaptic currents have a slower decay time when mediated by NR2b containing NMDA receptors compared to NR2a containing receptors (42). An NR1/NR2a/NR2b containing cell has a deactivation time course intermediate between that of the NR1/NR2a and NR1/NR2b, although other electrophysiological properties have not been tested for this configuration (13). These all have important implications for the action of these receptors on the cell body. These results suggest that the expression pattern of NR2b containing cells in the AVPV, a nucleus important in the regulation of female reproductive function, is changing with age, and thus supports that these changing receptors have a functional effect on the dysregulation of the reproductive axis observed with increased age. Studies reporting that the responsiveness of GnRH neurones to NMDA receptor analogues/antagonists is altered with age (3,20,43) are consistent with age-related changes in physiological properties of NMDA receptors. Our results provide a potential link between the structural changes in NMDA receptors and these age-associated functional consequences.

Age-related changes in AVPV are limited to specific cell phenotypes

Although total cell number in the AVPV was not determined (i.e. the present study focused only on those cells expressing NMDA receptors), our finding that AVPV volume did not change as a function of age or hormone treatment, nor were there any qualitatively apparent changes in cell size in either brightfield (DAB) or confocal (immunofluorescence) studies, suggests that the number of cells that comprise the AVPV remains static. This observation is further supported by other studies examining the AVPV, ventromedial nucleus, arcuate nucleus and medial preoptic area of the hypothalamus, in which no age-related change in neuronal cell number or regional volume has been found (28,44-46). Such a lack of wholesale cell loss in the hypothalamus with ageing is consistent with the suggestion that normal ageing is not accompanied by a generalised loss of neurones, but rather a change in the phenotype of existing neurones (47). Thus, our observed alterations in NMDA receptor subunit expression are likely the result of changes in the receptor stoichiometry itself, rather than changes to overall cell number in the AVPV.

Oestradiol interacts with the NMDA receptor

The ability of glutamate to activate the NMDA receptor is sensitive to oestradiol. Most electrophysiological work has focused on the hippocampus in which it was shown that oestradiol facilitates several NMDA-dependent markers of excitation and synaptic plasticity (e.g. dendritic spine density and synapse density) (48). In the hypothalamus, the presence of oestradiol increases NR2b mRNA expression in the preoptic area-anterior hypothalamus, whereas NR1 remains static (1). It also appears to affect the association of NR2b with neuronal nitric oxide synthase, a regulatory protein for nitric oxide and a neuromodulator of the reproductive axis (49). Furthermore, NR1 mRNA expression in the AVPV specifically increases with steroid hormone treatment (6), but an alternate study found that this did not translate to the level of the protein because this remained unchanged (14). Notably, receptor binding studies showed that oestradiol does not affect glutamate binding to the NMDA receptor in hypothalamus and cortex, suggesting a different mechanism of action other than receptor binding (50). In addition, a large percentage of NR1-containing cells in the AVPV also co-express ERα, suggesting that the same cells may mediate actions of both glutamate and oestradiol (7). Thus, the mechanisms by which oestradiol enhances glutamate actions on

the NMDA receptor remain to be elucidated, but likely involve actions on converging target cells.

In the present study, there was no effect of oestradiol on NR2b immunoreactive cell numbers. By contrast, confocal analysis of immuofluorescent fraction volume of NR1 alone, NR2b alone, and NR1 co-expressed with NR2b, showed an increase in NR2b fraction volume in oestradiol-vehicle treated rats, but not vehicle-vehicle or oestradiol-progesterone rats. Although there was an apparent increase in fraction volume of cells co-expressing NR1 with NR2b in the oestradiol-vehicle rats, this was not significant. The finding that oestradiol specifically increased the NR2b-immunofluorescent fraction volume in the AVPV supports potential interactions between oestrogens and NMDA receptor signalling. Taken together with the stereology data, in which there was no effect of oestradiol on the number or density of NR2b-immunoreactive cells, our data suggest that oestradiol enhances protein translation, ultimately resulting in an increased amount of protein expressed in each cell, but not an increase in the number of cells expressing this subunit. Functionally, this likely translates to an alteration in NMDA receptor function in the reproductive system.

Notably, this effect of oestradiol was not observed when rats were treated with progesterone, suggesting some reversal or mitigation of the effects of oestradiol by progesterone. We believe the timing of hormone treatment relative to euthanasia may underlie the differences between the oestradiol plus vehicle and the oestradiol plus progesterone groups. In the present study, ovariectomised rats were treated with oestradiol, followed 48 h later by progesterone or vehicle, with euthanasia occurring 24 h after progesterone. Progesterone treatment alters neuroendocrine signalling, such as the GnRH surge, in a manner that initially facilitates but then more rapidly terminates oestradiol's actions compared to oestradiol alone. In the absence of progesterone, the oestradiol-induced GnRH/LH surge is of lower amplitude but it is prolonged, resulting in a very different neuroendocrine environment. Future studies are being designed to euthanise rats earlier after progesterone administration, during the GnRH surge, aiming for a comparison with the results obtained in the present study.

Conclusions

Overall, the present study provides further evidence that the NMDA receptor subunit composition in the AVPV changes as function of age. The increase in NR1/NR2b fraction volume, along with a decline in the density of cells expressing NR2b, suggests a cell-specific change in receptor stoichiometry, likely resulting in functional effects exerted on the reproductive axis. In addition, oestradiol modulated the fraction volume of NR2b expression in the AVPV.

Further research is necessary to determine the specific functional consequences of this alteration. We hypothesise that this stoichiometric change results in an increased duration of the channel open period compared to NR2a-containing receptors, and thus may cause stimulation of inhibitory pathways, such as GABA, on the GnRH system. Consistent with this idea, Neal-Perry *et al.* (51) recently demonstrated that GABA levels in the hypothalamus are higher in middle-aged than in young rats. This would, in part, result in the observed age-associated decline in the activity of the reproductive axis. However, we do not exclude the possibility that age-associated alterations in NMDA receptor composition may be a mechanism whereby direct, indirect, or a combination of inputs, may result in age-associated changes to GnRH output, affecting overall reproductive function during senescence.

Acknowledgments

This work was supported by the NIH PO1 AG16765 and RO1 AG028051 to A.C.G. We thank Deena Walker for conducting the progesterone assays, and Weiling Yin and Kristin Reynolds for assistance on the animal care and procedures. We are grateful to Dr A. F. Parlow of the National Hormone and Pituitary Programme at NIDDK for providing LH assay reagents and Dr Michael Woller of the University of Wisconsin-Whitewater for conducting the LH RIA. Finally, we thank Dr Angela M. Bardo of The University of Texas at Austin Molecular Biology Core facility for extensive training and advice concerning confocal imaging and Imaris 5.7.0 analysis.

References

1. Mahesh VB, Brann DW. Regulatory role of excitatory amino acids in reproduction. Endocrine. 2005; 28:271–280. [PubMed: 16388116]
2. Gore AC. Gonadotropin-releasing hormone neurons, NMDA receptors, and their regulation by steroid hormones across the reproductive life cycle. Brain Res Brain Res Rev. 2001; 37:235–248. [PubMed: 11744089]
3. Brann DW, Mahesh VB. The aging reproductive neuroendocrine axis. Steroids. 2005; 70:273–283. [PubMed: 16080236]
4. Herman JP, Eyigor O, Ziegler DR, Jennes L. Expression of ionotropic glutamate receptor subunit mRNAs in the hypothalamic paraventricular nucleus of the rat. J Comp Neurol. 2000; 422:352–362. [PubMed: 10861512]
5. Eyigor O, Centers A, Jennes L. Distribution of ionotropic glutamate receptor subunit mRNAs in the rat hypothalamus. J Comp Neurol. 2001; 434:101–124. [PubMed: 11329132]
6. Gu G, Varoqueaux F, Simerly RB. Hormonal regulation of glutamate receptor gene expression in the anteroventral periventricular nucleus of the hypothalamus. J Neurosci. 1999; 19:3213–3222. [PubMed: 10191334]
7. Chakraborty TR, Ng L, Gore AC. Colocalization and hormone regulation of estrogen receptor alpha and N-methyl-D-aspartate receptor in the hypothalamus of female rats. Endocrinology. 2003; 144:299–305. [PubMed: 12488358]
8. Monyer H, Sprengel R, Schoepfer R, Herb A, Higuchi M, Lomeli H, Burnashev N, Sakmann B, Seeburg PH. Heteromeric NMDA receptors - molecular and functional distinction of subtypes. Science. 1992; 256:1217–1221. [PubMed: 1350383]
9. Monyer H, Burnashev N, Laurie DJ, Sakmann B, Seeburg PH. Developmental and regional expression in the rat brain and functional properties of 4 NMDA receptors. Neuron. 1994; 12:529–540. [PubMed: 7512349]
10. Kutsuwada T, Kashiwabuchi N, Mori H, Sakimura K, Kushiya E, Araki K, Meguro H, Masaki H, Kumanishi T, Arakawa M, Mishina M. Molecular diversity of the NMDA receptor channel. Nature. 1992; 358:36–41. [PubMed: 1377365]
11. Chen N, Luo T, Raymond LA. Subtype-dependence of NMDA receptor channel open probability. J Neurosci. 1999; 19:6844–6854. [PubMed: 10436042]
12. Sheng M, Cummings J, Roldan LA, Jan YN, Jan LY. Changing subunit composition of heteromeric NMDA receptors during development of rat cortex. Nature. 1994; 368:144–147. [PubMed: 8139656]
13. Vicini S, Wang JF, Li JH, Zhu WJ, Wang YH, Luo JH, Wolfe BB, Grayson DR. Functional and pharmacological differences between recombinant N-methyl-D-aspartate receptors. J Neurophysiol. 1998; 79:555–566. [PubMed: 9463421]
14. Chakraborty TR, Ng L, Gore AC. Age-related changes in estrogen receptor beta in rat hypothalamus: a quantitative analysis. Endocrinology. 2003; 144:4164–4171. [PubMed: 12933691]
15. Simerly RB. Wired for reproduction: organization and development of sexually dimorphic circuits in the mammalian forebrain. Annu Rev Neurosci. 2002; 25:507–536. [PubMed: 12052919]
16. Wiegand SJ, Terasawa E, Bridson WE, Goy RW. Effects of discrete lesions of preoptic and suprachiasmatic structures in the female rat. Alterations in the feedback regulation of gonadotropin secretion. Neuroendocrinology. 1980; 31:147–157. [PubMed: 6771669]

17. Wintermantel TM, Campbell RE, Porteous R, Bock D, Grone HJ, Todman MG, Korach KS, Greiner E, Perez CA, Schutz G, Herbison AE. Definition of estrogen receptor pathway critical for estrogen positive feedback to gonadotropin-releasing hormone neurons and fertility. Neuron. 2006; 52:271–280. [PubMed: 17046690]

18. Herbison AE. Estrogen positive feedback to gonadotropin-releasing hormone (GnRH) neurons in the rodent: the case for the rostral periventricular area of the third ventricle (RP3V). Brain Res Rev. 2008; 57:277–287. [PubMed: 17604108]

19. Maffucci JA, Walker DM, Ikegami A, Woller MJ, Gore AC. NMDA receptor subunit NR2b: effects on LH release and GnRH gene expression in young and middle-aged female rats, with modulation by estradiol. Neuroendocrinology. 2008; 87:129–141. [PubMed: 18025808]

20. Gore AC, Yeung G, Morrison JH, Oung T. Neuroendocrine aging in the female rat: the changing relationship of hypothalamic gonadotropin-releasing hormone neurons and N-methyl-D-aspartate receptors. Endocrinology. 2000; 141:4757–4767. [PubMed: 11108291]

21. Gore AC, Oung T, Yung S, Flagg RA, Woller MJ. Neuroendocrine mechanisms for reproductive senescence in the female rat: gonadotropin-releasing hormone neurons. Endocrine. 2000; 13:315–323. [PubMed: 11216643]

22. Adams MM, Oung T, Morrison JH, Gore AC. Length of postovariectomy interval and age, but not estrogen replacement, regulate N-methyl-D-aspartate receptor mRNA levels in the hippocampus of female rats. Exp Neurol. 2001; 170:345–356. [PubMed: 11476600]

23. National Research Council. Guide for the Care and Use of Laboratory Animals. National Academies Press; Washington, DC: 1996.

24. Gore AC, Oung T, Woller MJ. Age-related changes in hypothalamic gonadotropin-releasing hormone and N-methyl-D-aspartate receptor gene expression, and their regulation by oestrogen, in the female rat. J Neuroendocrinol. 2002; 14:300–309. [PubMed: 11963827]

25. Gore AC, Roberts JL. Regulation of gonadotropin-releasing hormone gene expression in the rat during the luteinizing hormone surge. Endocrinology. 1995; 136:889–896. [PubMed: 7867597]

26. Iglewiicz, B.; Hoaglin, DC. How to Detect and Handle Outliers. ASQC Quality Press; Milwaukee, WI: 1993.

27. Adams MM, Fink SE, Janssen WG, Shah RA, Morrison JH. Estrogen modulates synaptic N-methyl-D-aspartate receptor subunit distribution in the aged hippocampus. J Comp Neurol. 2004; 474:419–426. [PubMed: 15174084]

28. Chakraborty TR, Hof PR, Ng L, Gore AC. Stereologic analysis of estrogen receptor alpha (ER alpha) expression in rat hypothalamus and its regulation by aging and estrogen. J Comp Neurol. 2003; 466:409–421. [PubMed: 14556297]

29. Swanson, LW. Brain Maps: Structure of the Rat Brain. 3rd edn.. Elsevier; New York, NY: 2003.

30. Paxinos, G.; Kus, L.; Ashwell, KWS.; Watson, C. Chemoarchitectronic Atlas of the Rat Forebrain. Academic Press; San Diego, CA: 1999.

31. Schmitz C, Hof PR. Recommendations for straightforward and rigorous methods of counting neurons based on a computer simulation approach. J Chem Neuroanat. 2000; 20:93–114. [PubMed: 11074347]

32. West MJ, Slomianka L, Gundersen HJ. Unbiased stereological estimation of the total number of neurons in the subdivisions of the rat hippocampus using the optical fractionator. Anat Rec. 1991; 231:482–497. [PubMed: 1793176]

33. Siegel SJ, Brose N, Janssen WG, Gasic GP, Jahn R, Heinemann SF, Morrison JH. Regional, cellular, and ultrastructural distribution of N-methyl-D-aspartate receptor subunit 1 in monkey hippocampus. Proc Natl Acad Sci USA. 1994; 91:564–568. [PubMed: 8290563]

34. Hana V, Haluzik M, Schreiber V. Independence of estrogen-induced pituitary proliferation on local IGF-I mRNA and EGF mRNA expression. Modifying effects of tamoxifen and terguride. Physiol Res. 1998; 47:125–131. [PubMed: 9706996]

35. Abech DD, Moratelli HB, Leite SC, Oliveira MC. Effects of estrogen replacement therapy on pituitary size, prolactin and thyroid-stimulating hormone concentrations in menopausal women. Gynecol Endocrinol. 2005; 21:223–226. [PubMed: 16316844]

36. Adams JM, Tan SL, Wheeler MJ, Morris DV, Jacobs HS, Franks S. Uterine growth in the follicular phase of the spontaneous ovulatory cycles and during luteinizing hormone-releasing

hormone-induced cycles in women with normal or polycystic ovaries. Fertil Steril. 1988; 49:52–55. [PubMed: 3275552]

37. Stygar D, Muravitskaya N, Eriksson B, Eriksson H, Sahlin L. Effects of SERM (selective estrogen receptor modulator) treatment on growth and proliferation in the rat uterus. Reprod Biol Endocrinol. 2003; 1:40. [PubMed: 12777179]
38. Miller BH, Gore AC. N-Methyl-D-aspartate receptor subunit expression in GnRH neurons changes during reproductive senescence in the female rat. Endocrinology. 2002; 143:3568–3574. [PubMed: 12193572]
39. Saito Y, Tsuzuki K, Yamada N, Okado H, Miwa A, Goto F, Ozawa S. Transfer of NMDAR2 cDNAs increases endogenous NMDAR1 protein and induces expression of functional NMDA receptors in PC12 cells. Brain Res Mol Brain Res. 2003; 110:159–168. [PubMed: 12591153]
40. Luo J, Wang Y, Yasuda RP, Dunah AW, Wolfe BB. The majority of N-methyl-D-aspartate receptor complexes in adult rat cerebral cortex contain at least three different subunits (NR1/NR2A/NR2B). Mol Pharmacol. 1997; 51:79–86. [PubMed: 9016349]
41. Erreger K, Dravid SM, Banke TG, Wyllie DJ, Traynelis SF. Subunit-specific gating controls rat NR1/NR2A and NR1/NR2B NMDA channel kinetics and synaptic signalling profiles. J Physiol. 2005; 563(Pt 2):345–358. [PubMed: 15649985]
42. Flint AC, Maisch US, Weishaupt JH, Kriegstein AR, Monyer H. NR2A subunit expression shortens NMDA receptor synaptic currents in developing neocortex. J Neurosci. 1997; 17:2469–2476. [PubMed: 9065507]
43. Bonavera JJ, Swerdloff RS, Sinha Hakim AP, Lue YH, Wang C. Aging results in attenuated gonadotropin releasing hormone-luteinizing hormone axis responsiveness to glutamate receptor agonist N-methyl-D-aspartate. J Neuroendocrinol. 1998; 10:93–99. [PubMed: 9535055]
44. Madeira MD, Ferreira-Silva L, Ruela C, Paula-Barbosa MM. Differential effects of the aging process on the morphology of the hypothalamic ventromedial nucleus of male and female rats. Neurosci Lett. 2001; 314:73–76. [PubMed: 11698150]
45. Madeira MD, Andrade JP, Paula-Barbosa MM. Hypertrophy of the ageing rat medial preoptic nucleus. J Neurocytol. 2000; 29:173–197. [PubMed: 11428048]
46. Leal S, Andrade JP, Paula-Barbosa MM, Madeira MD. Arcuate nucleus of the hypothalamus: effects of age and sex. J Comp Neurol. 1998; 401:65–88. [PubMed: 9802701]
47. Finch CE. Neurons, glia, and plasticity in normal brain aging. Neurobiol Aging. 2003; 24(Suppl 1):S123–S127. [PubMed: 12829120]
48. Spencer JL, Waters EM, Romeo RD, Wood GE, Milner TA, McEwen BS. Uncovering the mechanisms of estrogen effects on hippocampal function. Front Neuroendocrinol. 2008; 29:219–237. [PubMed: 18078984]
49. d'Anglemont de Tassigny X, Campagne C, Dehouck B, Leroy D, Holstein GR, Beauvillain JC, Buee-Scherrer V, Prevot V. Coupling of neuronal nitric oxide synthase to NMDA receptors via postsynaptic density-95 depends on estrogen and contributes to the central control of adult female reproduction. J Neurosci. 2007; 27:6103–6114. [PubMed: 17553983]
50. Brann DW, Zamorano PL, Chorich LP, Mahesh VB. Steroid hormone effects on NMDA receptor binding and NMDA receptor mRNA levels in the hypothalamus and cerebral cortex of the adult rat. Neuroendocrinology. 1993; 58:666–672. [PubMed: 7907400]
51. Neal-Perry GS, Zeevalk GD, Shu J, Etgen AM. Restoration of the luteinizing hormone surge in middle-aged female rats by altering the balance of GABA and glutamate transmission in the medial preoptic area. Biol Reprod. 2008; 79:878–888. [PubMed: 18667749]

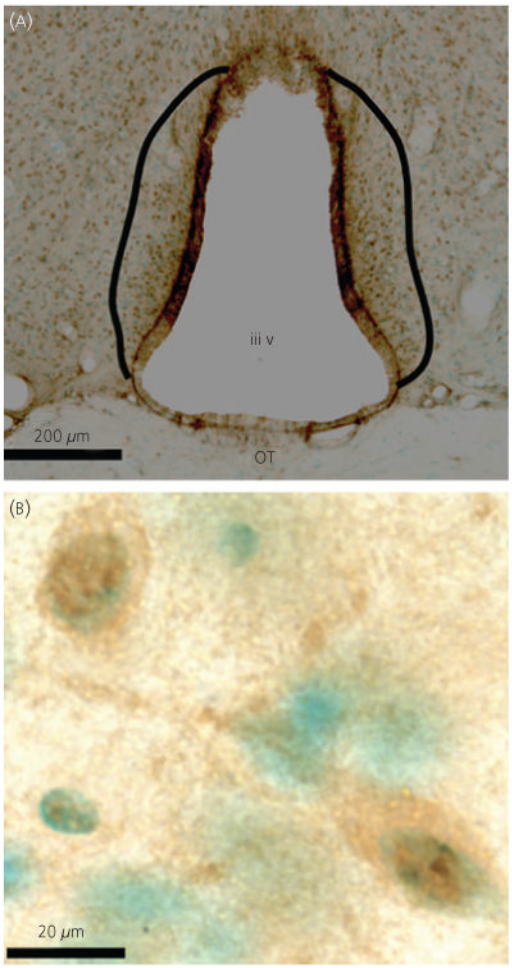

Fig. 1.

Representative micrographs of NR2b immunoreactivity at low (× 10; A) and high (× 100; B) magnification. (A) The anteroventral periventricular region examined is defined by the solid black lines. (B) Individual NR2b immunoreactive cells (brown diamino benzidene label), counterstained with methyl green (green nuclei). OT, optic tract; iiiv, third ventricle.

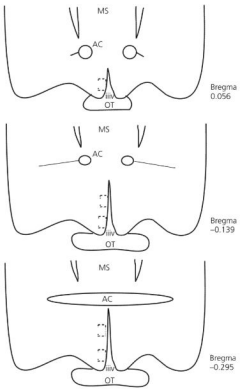

Fig. 2.

Depiction of the sampling methodology used for the confocal analysis of NR1 and NR2b immunofluorescence in the anteroventral periventricular region from rostral (top) to caudal (bottom). The dotted squares represent the approximate area scanned for each tissue section. The anterior-posterior distances to Bregma are shown to the right of each depicted section, as noted by Paxinos *et al.* (30). OT, optic tract; iiiv, third ventricle; MS, medial septum; AC, anterior commissure.

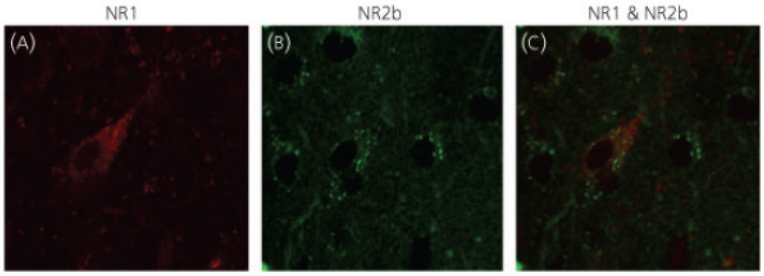

Fig. 3.

Representative confocal micrographs, taken at × 40 magnification with 1.84 zoom, on the confocal microscope. Micrographs demonstrate immunofluorescent labelling of cells in the anteroventral periventricular: (A) NR1, (B) NR2b and (C) an overlay of NR1 and NR2b. Note that the tonal curves were adjusted relatively equally using the curve function in Adobe Photoshop (Adobe Systems Inc., San Jose, CA, USA) in all panels to facilitate viewing the immunofluorescent labelling. However, such manipulations were not performed during the actual analysis. In addition, micrographs for visual presentation were taken at a higher intensity and resolution than those used during data acquisition to enable better visualisation of the NR2b-immunoreactive cells.

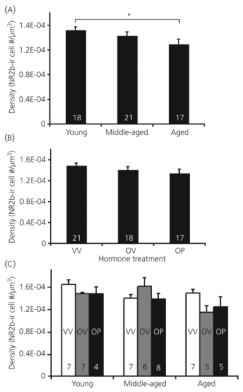

Fig. 4.

Stereologic analyses of NR2b immunoreactive (-ir) cell density. The density of NR2b immunoreactive cells decreases as a function of age in the anteroventral periventricular region (A; P = 0.024), but does not change with steroid hormone treatment (B), nor is there an interaction of these variables (C). Hormone treatment groups are: VV, vehicle, vehicle; OV, 17*β*-oestradiol, vehicle; OP, 17*β*-oestradiol, progesterone. The numbers at the bottom of each bar represent the number of rats per group. *P < 0.05.

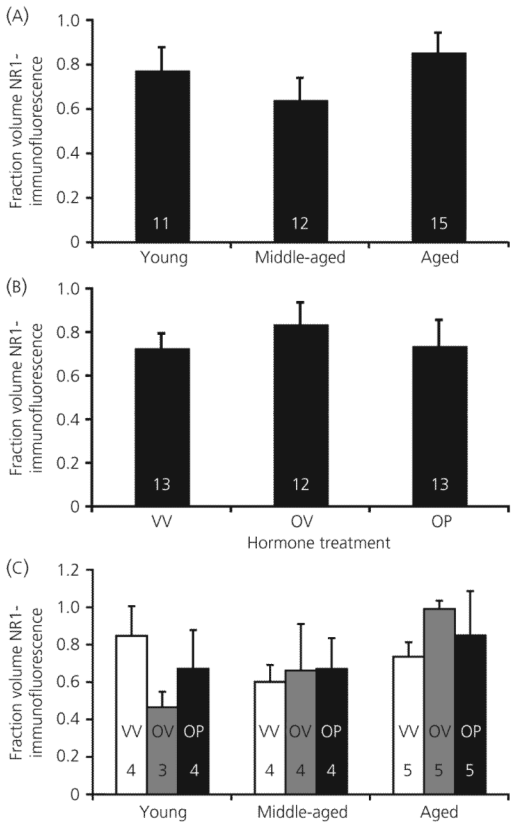

Fig. 5.

Confocal analysis of the fraction volume of immunofluorescent NR1 in the anteroventral periventricular region. Fraction volume of NR1 does not change as a function of age (A) or steroid hormone treatment (B), nor is there an interaction of these variables (C). Hormone treatment groups are: VV, vehicle, vehicle; OV, 17*β*-oestradiol, vehicle; OP, 17*β*-oestradiol, progesterone. The numbers at the bottom of each bar represent the number of rats per group.

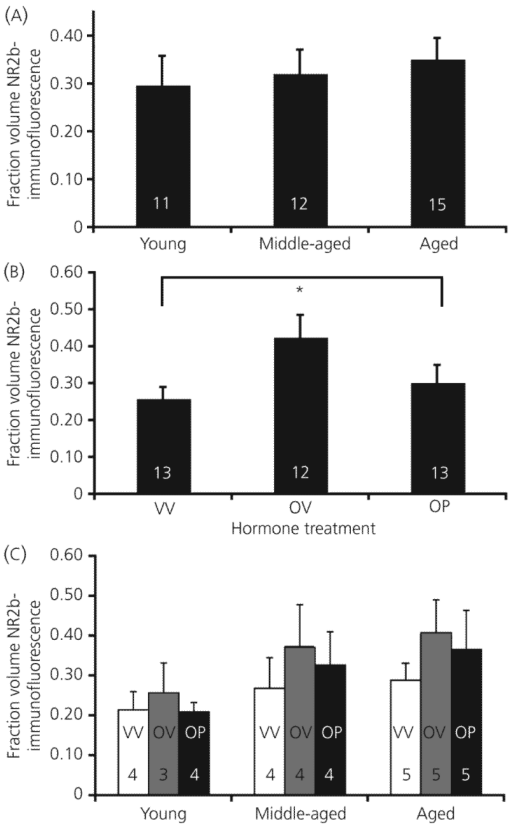

Fig. 6.

The fraction volume of immunofluorescent NR2b in the AVPV does not change as a function of age (A), but does increase with oestradiol treatment (B). There is no interaction of these variables (C). Hormone treatment groups are: VV, vehicle, vehicle; OV, 17*β*-oestradiol, vehicle; OP, 17*β*-oestradiol, progesterone. The numbers at the bottom of each bar represent the number of rats per group. *P < 0.05.

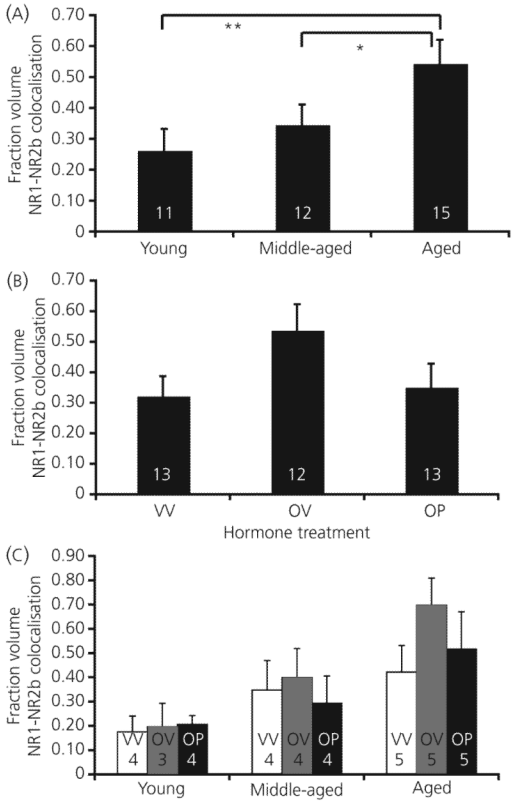

Fig. 7.

The fraction volume of NR1 and NR2b colocalised in the AVPV increases with age (A) but not hormone treatment (B), and these two variables do not interact (C). Hormone treatment groups are: VV, vehicle, vehicle; OV, 17*β*-oestradiol, vehicle; OP, 17*β*-oestradiol, progesterone. The numbers at the bottom of each bar represent the number of rats per group. *P < 0.05, **P < 0.01.

Table 1

Serum Hormone Levels of Young, Middle-aged, and Aged Ovariectomised Female Rats

Age	Hormone treatment	LH (ng/ml)	Progesterone (ng/ml)
Young	Vehicle/vehicle	17.71 ± 1.92 (n = 8)	8.97 ± 2.83 (n = 8)
	Oestradiol/vehicle	8.37 ± 0.37 (n = 6)	10.51 ± 2.73 (n = 8)
	Oestradiol/progesterone	8.00 ± 0.88 (n = 6)	15.48 ± 2.34 (n = 7)
Middle-aged	Vehicle/vehicle	8.34 ± 0.35 (n = 7)	7.47 ± 1.02 (n = 7)
	Oestradiol/vehicle	10.68 ± 1.58 (n = 8)	10.75 ± 2.17 (n = 8)
	Oestradiol/progesterone	6.03 ± 0.24 (n = 7)	15.51 ± 2.17 (n = 8)
Aged	Vehicle/vehicle	3.27 ± 0.56 (n = 6)	7.24 ± 1.36 (n = 10)
	Oestradiol/vehicle	4.60 (n = 2)	11.23 ± 2.46 (n = 6)
	Oestradiol/progesterone	3.28 ± 0.62 (n = 8)	15.52 ± 7.33 (n = 8)

Luteinising hormone (LH) values showed a main effect of age ($P < 0.0001$) and hormone treatment ($P < 0.001$), and a significant interaction ($P < 0.001$). Specifically, the young-vehicle/vehicle rats had significantly higher LH levels than all other groups ($P < 0.005$). Progesterone levels did not vary with age ($P = 0.843$), but were significantly different between steroid hormone treatments ($P < 0.001$), with levels significantly highest in the progesterone treated rats. Mean ± SEM are shown (except for the aged oestradiol/vehicle group for which serum samples of only two rats could be obtained for LH).

Table 2

Pituitary Weight and Uterine Diameter of Young, Middle-aged, and Aged Ovariectomised Female Rats

Age	Hormone treatment	Pituitary weight (normalised to body weight)	Uterine diameter (mm)
Young	Vehicle/vehicle	$4.75 \times 10^{-5} \pm 1.88 \times 10^{-6}$ (n = 4)	1.36 ± 0.10 (n = 8)
	Oestradiol/vehicle	$6.18 \times 10^{-5} \pm 2.59 \times 10^{-6}$ (n = 7)	4.83 ± 0.37 (n = 7)
	Oestradiol/progesterone	$6.07 \times 10^{-5} \pm 3.87 \times 10^{-6}$ (n = 7)	8.34 ± 0.73 (n = 7)
Middle-aged	Vehicle/vehicle	$4.96 \times 10^{-5} \pm 2.70 \times 10^{-6}$ (n = 7)	2.13 ± 0.22 (n = 8)
	Oestradiol/vehicle	$5.58 \times 10^{-5} \pm 3.54 \times 10^{-6}$ (n = 4)	3.86 ± 0.99 (n = 8)
	Oestradiol/progesterone	$6.80 \times 10^{-5} \pm 3.67 \times 10^{-6}$ (n = 4)	4.91 ± 0.41 (n = 8)
Aged	Vehicle/vehicle	$5.81 \times 10^{-5} \pm 1.26 \times 10^{-6}$ (n = 5)	2.39 ± 0.38 (n = 7)
	Oestradiol/vehicle	$7.93 \times 10^{-5} \pm 2.28 \times 10^{-6}$ (n = 4)	4.60 ± 0.25 (n = 2)
	Oestradiol/progesterone	$6.09 \times 10^{-5} \pm 1.08 \times 10^{-6}$ (n = 4)	4.10 ± 0.39 (n = 8)

Pituitary weights and uterine diameter, the latter an index of the uterotrophic effect of oestradiol, were measured in post-mortem rats following perfusion. Pituitary weights did not vary significantly with age, but had a trend for an effect of hormone treatment ($P = 0.051$). In general, pituitaries were smaller in the vehicle/vehicle groups compared to the oestradiol/vehicle or oestradiol/progesterone groups. Uterine diameter measurements showed no age-associated differences, but there was a main effect of hormone treatment ($P < 0.001$). Specifically, uterine diameter was larger in oestradiol/vehicle and oestradiol/progesterone than in vehicle/vehicle rats. Data are the mean ± SEM.